J3.2 TRANSPORT AND CHEMICAL TRANSFORMATIONS INFLUENCED BY SHALLOW CUMULUS OVER LAND

Jordi Vilà-Guerau de Arellano *
Meteorlogy and Air Quality Section, Wageningen University, The Netherlands
Si-Wan Kim †, Mary C. Barth and Edward G. Patton
Mesoscale and Microscale Meteorology Division, National Center for Atmospheric Research, USA

1. INTRODUCTION

Shallow cumulus (Cu) clouds over land are a manifestation of convection in the atmospheric boundary layer (ABL). Their formation and evolution depend strongly on the partitioning between the sensible- and latent-heat fluxes, the wind shear and the vertical structure of the thermodynamic state variables. Because the structure of the boundary layer with shallow cumulus differs from the clear boundary layer, the dynamics driven by the presence of Cu leads to variations of the boundary layer characteristics, which also determines the evolution and distribution of atmospheric reactive compounds. Shallow cumulus clouds generally form in synoptically high pressure regions which are conducive to the formation and accumulation of both passive and photochemically generated pollutants in the boundary layer because of the low wind speeds, the intensification of capping inversions, and high insolation. As a consequence, shallow Cu can affect the variability of chemical species in four ways: (a) the enhancement of vertical transport of the chemical species, (b) the turbulent mixing of atmospheric compounds, (c) the perturbation of ultraviolet radiation, and therefore of photodissociation rates, below, in and above the clouds and (d) the chemical reactions occurring within the cloud droplets. In this study, we focus on the first three of these effects.

Although shallow Cu clouds are a common feature in atmospheric boundary layers over land, little is known about their role on the transport, mixing, and photodissociation of chemical compounds. Shallow cumulus have the potential to enhance vertical transport of atmospheric compounds such that the compounds reach higher altitudes. The vertical transport is dependent on the strength of the clouds and on the temperature capping inversion. Field observations (Ching and Alkezweeny, 1986; Ching et al., 1988; Baumann et al., 2000; Angevine, 2005) have shown that the presence of shallow cumuli leads to a reduction of the pollutants in the sub-cloud layer due to the enhanced vertical transport by cumulus clouds.

In these cloudy boundary layers, highly turbulent regions are localized in the cloud updraft whereas the compensating subsidence regions are characterized by less turbulent downward motions. As a result, reactive species may become segregated such that turbulent mixing controls the reactivity of second-order chemical reactions (Schumann, 1989; Molemaker and Vilà-Guerau de Arellano, 1998). This limitation of reactivity is particularly important if the chemical time scales are of similar order to the turbulent transport time scale.

Finally, clouds disrupt the ultraviolet radiation field by perturbing the contributions of direct and diffuse radiation. In a seminal paper, Madronich (1987) investigated how cloud layers modify the vertical profiles of actinic flux, and therefore the photodissociation rates. He showed that compared to the clear-sky photodissociation values, the perturbed photodissociation rates decrease in the sub-cloud layer, increase almost linearly in the cloud, and are enhanced above the cloud. In a previous numerical study on the reactions in a homogeneous stratocumulus cloud deck, Vilà-Guerau de Arellano and Cuijpers (2000) showed that the influence of the physical processes (turbulence and radiation) leads to an increase of the reactant's concentration gradient and consequently to a departure from photochemical equilibrium.

Our objective is to study the roles of transport and radiation in fair weather cumulus on reactive species. By means of a large-eddy simulation technique, we investigate the daytime evolution of reactive species in shallow Cu. We define a series of numerical experiments to (1) investigate the modification on the reactant distribution because of the enhancement of the boundary layer growth (defined by the cloud top height) by shallow Cu, (2) test the validity of current parameterizations of the vertical transport, (3) quantify the control of turbulent mixing on the species reactivity and (4) study how perturbed photodissociation rates by clouds affect the transformation of species. The study is

* *Corresponding author address:* Jordi Vilà-Guerau de Arellano, Meteorlogy and Air Quality Section, Duivendaal 2, 6701 AP Wageningen, The Netherlands, e-mail:jordi.vila@wur.nl

† *Current affiliation:* Earth System Research Laboratory, National Oceanic and Atmospheric Organization

based on the simulations carried out by the following two large-eddy simulation (LES) models: National Center for Atmospheric Research (NCAR) and Wageningen University Research (WUR). The intercomparison of the two codes allows us to assess the use of the LES technique to calculate diagnostic fields for turbulent reacting flows. In the absence of reliable and systematic observational field data, the LES method could provide a unique data base to study the influence of cloudy boundary layer dynamics on chemical transformations. Not only does this work provide a systematic study of turbulent photochemical reacting flows in the presence of shallow cumulus clouds, but it is the first time that an intercomparison of reactive chemistry in the LES framework is being conducted. An extensive discussion of the results and the simulation intercomparison can be found at Vilà-Guerau de Arellano et al. (2005).

2. DESCRIPTION OF THE CASE: OBSERVATIONS AND NUMERICAL EXPERIMENTS

Our study is based on the meteorological situation discussed by Brown et al. (2002). The same case has also been used to test the ability of single column cloud models to reproduce shallow cumulus over land (Lenderink et al., 2005). Below, we provide a brief description of the observations, the set up of the numerical experiment, and the validation of the diagnostic fields associated with the thermodynamic and reactant variables.

A cloudy boundary layer characterized by the presence of shallow cumulus was observed on 21 June 1997 at the Southern Great Plains (SGP) site of the Atmospheric Radiation Measurement (ARM) program in Oklahoma. Based on the surface and on the upper air observations, Brown et al. (2002) proposed an idealized numerical experiment to study the dynamics of shallow cumulus convection over land by means of large-eddy simulations. The case was characterized by a strong diurnal cycle of both sensible and latent heat fluxes, which were the surface forcings for the formation of clouds. The friction velocity follows a weak diurnal cycle with a maximum value of 0.54 $m\ s^{-1}$ and a minimum value of 0.45 $m\ s^{-1}$. The observed radiosonde vertical profiles of potential temperature showed first a stable boundary layer at 05.30 LT (11.30 UTC) which rapidly became a well mixed boundary layer by 08.30 LT (14.30 LT). Measurements of the cloud fraction showed the presence of scattered clouds after 08.30 LT with cloud cover ranging from 0.2 to 0.45. The cloud base height was around 1000 m after this time.

Two large-eddy simulation (LES) codes are used to study the transport and the transformation of reactants in a cloudy boundary layer: the WUR-LES code (Cuijpers and Duynkerke, 1993; Siebesma and Cuijpers, 1995; Vilà-Guerau de Arellano and Cuijpers, 2000) and the NCAR-LES code (Moeng, 1984; Sullivan et al., 1996; Patton et al., 2005). Both codes participated previously at the intercomparison exercise described in Brown et al. (2002). The initial conditions and surface forcing are the same as those prescribed by Brown et al. (2002) except that the initial potential temperature has been slightly modified to simulate a cloud top height that rises faster than their standard case. Surface fluxes of heat and moisture vary with time similar to those measured. The only other external forcing is a prescribed westerly geotropic wind equal to 10 $m\ s^{-1}$. Small external tendencies representing the advection of heat and moisture are not included. The model domain size is $6400\ m$ x $6400\ m$ x $4400\ m$ with a horizontal grid length equal to 66.7 m and a vertical grid length equal to 40 m. The simulations are integrated from 05.30 LT to 18.30 LT.

The chemical system is based on the atmospheric cycle of nitrogen dioxide, nitric oxide, and ozone. By using a simple chemical system, the influence of shallow cumulus on the transport of the species and on the photodissociation rates below, in and above the clouds can be clearly determined. The LES codes include the following two reactions:

$$NO_2 \xrightarrow{j} NO + O_3 \tag{1}$$

$$NO + O_3 \xrightarrow{k} NO_2, \tag{2}$$

where j and k are first- and second-order chemical reaction rates, respectively. The initial mixing ratio profiles of NO_2, NO and O_3 in the mixed layer are: 2 ppb, 1 ppb and 20 ppb. At the free troposphere, the mixing ratio of NO_2 and NO is zero and the mixing ratio of O_3 is 30 ppb. We also simulate an inert tracer whose initial profile is zero. The surface fluxes are constant with time using the following values: inert tracer (0.1 $ppb\ m\ s^{-1}$), NO_2 (0.1 $ppb\ m\ s^{-1}$), NO (0.05 $ppb\ m\ s^{-1}$) and O_3 (0.0 $ppb\ m\ s^{-1}$). The magnitude of the NO_2 and NO fluxes are fairly large in order to quickly obtain chemical equilibrium in the production and destruction of the three species, *i.e.* $\Phi = (k\ NO\ O_3)/(j\ NO_2) = 1$. By varying the values of j and k, one can study how the control of turbulence and the departure of chemical equilibrium influences the reactivity of the system. In the control simulation we use $j = 8.3 \times 10^{-3}$ (s^{-1}) and $k = 4.75 \times 10^{-4}$ $(ppb\ s^{-1})$.

An important aspect of this study is to investigate the modification of the photolysis rates by the presence of clouds. Because clouds alter the different proportions of direct and diffuse ultraviolet radiation, the actinic flux (and therefore the pho-

tolysis rates) has different values below, in, and above the clouds (Madronich, 1987). We have implemented this effect by calculating at every time step a factor below and above the clouds and by applying this factor to the clear sky value of the photolysis rate j_{clear} following Chang et al. (1987):

$$j_{clouds} = F\, j_{clear} \tag{3}$$

Above the cloud, the factor (F) is defined as:

$$F = 1 + \alpha\,(1 - t_r)\,cos(\chi_o). \tag{4}$$

While, below the cloud, F is defined as:

$$F = 1.6\,t_r\,cos(\chi_o). \tag{5}$$

Here, t_r is the energy transmission coefficient for normally incident light, χ_o is the solar zenith angle, and α is a reaction dependent coefficient (for nitrogen dioxide α=1.2). To simplify the calculation, a linear interpolation is assumed inside the cloud. Based on measurements of j_{NO_2} (Früh et al., 2000), the linear interpolation assumption likely overestimates the photolysis rate in the middle to lower regions of the cloud while underestimates the photolysis rate near cloud top.

The energy transmission coefficient t_r depends on the cloud optical depth and a scattering phase function asymmetry factor (f) equal to 0.86 for the typical cloud particle size ranges under study (Joseph et al., 1976). The expression reads:

$$t_r = \frac{5\,-\,e^{-\tau}}{[4\,+\,3\tau(1-f)]}. \tag{6}$$

The cloud optical depth (τ) is calculated according to the expression given by (Stephens, 1984)

$$\tau = \frac{3}{2}\frac{W}{\rho_l}\,r_e^{-1}, \tag{7}$$

where W is the vertically integrated liquid water ($kg\,m^{-2}$), ρ_l is the water density ($kg\,m^{-3}$) and r_e is the effective radius. Here, we have used a constant value of $r_e = 10\ \mu m$. For clouds characterized by values of $\tau < 5$ and for regions between clouds, we have assumed the photolysis rate of clear sky conditions. Regions between clouds may actually have enhanced photolysis rates due to cloud lateral scattering. Here, we are simply investigating the importance of cloud scattering in the cloud column. Our control simulation includes the modification of photolysis rates due to cloud scattering, while a sensitivity simulation excludes this effect on the chemistry.

3. RESULTS AND DISCUSSION

A thorough discussion on the evaluation of the intercomparison and the role of shallow cumulus on the transport and chemical transformation on chemical species can be found at Vilà-Guerau de Arellano et al. (2005). Here, we only focus our discussion on two relevant aspects: the enhancement of the vertical transport and the disruption of the photostationary state due to the combined effect of cloud turbulent convection in the cloud and the perturbed photolysis rate (j) above, in and below the cloud.

3.1 *Vertical enhancement*

Fair weather cumuli strongly modify the boundary layer structure by deepening its height, which in turn transports the sub-cloud compounds to the cloud layer. In order to investigate the impact of clouds on the distribution of atmospheric compounds, we conduct an additional LES experiment where shallow cumulus clouds do not form (i.e. clear sky conditions). In this experiment, we prescribe the same initial and boundary conditions as in the cloud simulation except that we reduce the initial profile of the total water mixing ratio by 3 $g\,kg^{-1}$.

Figure 1 shows the time evolution of the vertical profile of an inert species emitted at the surface for the cloud simulation (CL) and the clear sky simulation (CS). Similar evolution profiles are found for the emitted reactive species NO and NO_2. Notice that clouds start to form at around 10 LT (figure 1a). The enhancement of the vertical transport compared with the simulations where clouds are not formed (figure 1b) results in an increase of the mixing ratio in the cloud layer. It has to be mentioned that due to the inversion characteristics at the top of the CBL there is very little exchange between the CBL and the free troposphere in the situation being study.

We calculate the difference (in $\%$) of the mixing ratio (figure 2) between the simulation with clouds (CL) and without clouds (CS). This difference is normalized by the volume averaged mixing ratio calculated in the CS situation. As a reference of the distinct evolution of the two atmospheric boundary layers, we show the cloud top and cloud base height (CL case) and the boundary layer height (h) in the CS case. The h is calculated using the local gradient method (Sullivan et al., 1996) which determines the local inversion height based on the maximum of the liquid water potential temperature. As is seen in the figure, the transport of compounds to higher height results in a reduction of around 10$\%$ in the mixing ratio values in the dry CBL (CS) and in the subcloud layer (CL case). In consequence, larger values are found in the cloud layer (an increase of 15$\%$ in the middle of the cloud. Similar behaviour is found for the nitric oxide and nitrogen dioxide. The dilution of species has a particular impact on

reactants with a relatively small mixing ratio (in our case $NO,\ NO_2\ <\ O_3$), and it could lead to deviations in their diurnal variability.

We further examine the transport per unit of time by integrating the flux divergence term included in the conservation equation of the atmospheric compound. For instance, for nitrogen dioxide, we obtain values ranging from 1 ppb/hr at cloud onset to 0.2 ppb/hr once the cloud has fully developed. After 18 LT and when convective turbulence begins to decay, the increased dilution in the sub-cloud layer and the larger mixing ratio in the cloud layer persists (figure 2). Therefore, the presence of shallow cumulus can have an impact on the initial mixing ratio levels in the stable boundary layer and the residual layer which can influence the evolution of the nocturnal atmospheric chemistry.

3.2 *Departure from the photostationary steady state*

One of the main goals of this investigation was to study the combined effect of radiation and turbulence on the chemistry, and more in particular if chemical equilibrium is controlled by these physical processes. In order to investigate this effect, we set up two numerical experiments: the first one takes into account the perturbation of the j-values by clouds using expression (3) (j_{cloudy}). The second one assumes a constant photolysis with height and time and consequently the photodissociation rates are not perturbed by the Cu (j_{clear}). By calculating the differences of the instantaneous fields of the mixing ratio in both numerical experiments, we find differences up to a 40% below the cloud base height and up to 20% close to cloud top, which indicates a large variability in the reactant distribution, an important aspect in the interpretation of the chemical processes in and around clouds. These differences are dependent on the capacity of the vertical transport to smooth out the gradients created by the perturbed photodissociation rates, i.e. depending on the Damköhler number defined as ($Da = \tau_t/\tau_c$). For turbulent reacting flows characterized by values $Da \sim 1$ and larger, we find that turbulence is unable to decrease the mixing ratio gradients created by the different photodissociation rates below, in and above the cloud. It is important to mention that these differences are significantly reduced to values of $\sim$1% when averaged over the cloudy boundary layer in both space and time.

A variable that can quantify the effect of the physical processes (turbulence and radiation) on the atmospheric chemistry is the photostationary state equilibrium defined as $\Phi = (k\ NO\ O_3)/(j\ NO_2) = 1$. In Fig. 3, we show that the deviations of Φ can occur below, in and above the cloud. The calculation is based on the instantaneous mixing ratio values. Deviations from 1 indicate that the $j-$perturbation by clouds prevents to reach chemical equilibrium. Departures from the chemical equlibrium are larger below the cloud that in the cloud. Notice also that the spatial pattern of Φ is not uniform which confirm the existence of mixing ratio gradients in the cloud. Aircraft observations taken above the Netherlands under cloudy conditions also show a similar vertical profile of the photostationary state (van Weele and Duynkerke, 1993).

In the sub-cloud layer, the photostationary state is more than 50 $\%$ higher than the equlibrium value due to the decrease of the photodissociation rate. However, in both the cloud and sub-cloud layer there are also regions with $\Phi > 1$ and $\Phi < 1$. A possible explanation, still to be confirmed, can be based with inefficient mixing among the reactants within these regions and in consequence the chemical equilibrium has not been reached.

In concluding, the numerical study presented here shows that the presence of shallow cumulus influences the distribution and evolution of reactants by: (a) modifying the characteristics of the boundary layer: increasing the depth of the ABL depth and enhancing the vertical transport and (b) perturbing the radiative field and therefore the photolysis rate. As a result, the diurnal and nocturnal spatial characteristics of the reactants are largely determined by the presence of these boundary layer clouds.

REFERENCES

Angevine, W. M., 2005: An integrated turbulence scheme for boundary layers with shallow cumulus applied to pollutant transport. *J. Appl. Meteorol.*, **44**, 1436–1452.

Baumann, K., E. J. Willimas, W. M. Angevine, J. M. Roberts, R. B. Norton, G. J. Frost, F. C. Fehsenfeld, S. R. Springston, S. B. Bertman, and B. Hartsell, 2000: Ozone production and transport in Nashville, Tennessee: results from the 1994 study at New Hendersonville. *J. Geophys. Res.*, **105**, 9137–9153.

Brown, A. R., R. T. Cederwall, A. Chlond, P. G. Duynkerke, J. Golaz, J. M. Khairoutdinov, D. Lewellen, A. Lock, M. K. Macveen, C. Moeng, R. A. J. Neggers, A. P. Siebesma, and B. Stevens, 2002: Large-eddy simulation of the diurnal cycle of shallow cumulus convection over land. *Quart. J. Roy. Meteorol. Soc.*, **128(B)**, 1075–1094.

Chang, J., R. Brost, I. Isaksen, S. Madronich, P. Middleton, W. Stockwell, and C.J.Walcek, 1987: A three-dimensional eulerian acid deposition model: physical concepts and formulation. *J. Geophys. Res.*, **92**, 14681–14700.

Ching, J. K. S. and A. J. Alkezweeny, 1986: Trace study of vertical exchange by cumulus clouds. *J. Clim. and Appl. Meteorol.*, **25**, 1702–1711.

Ching, J. K. S., S. T. Shipley, and E. V. Browell, 1988: Evidence for cloud venting of mixed layer ozone and aerosols. *Atmos. Environ.*, **22**, 225–242.

Cuijpers, J. W. M. and P. G. Duynkerke, 1993: Large eddy simulations of trade wind with cumulus clouds. *J. Atmos. Sci.*, **50**, 3894–3908.

Früh, B., T. Trautmann, M. Wendisch, and A. Keil, 2000: Comparison of observed and simulated NO_2 photodissociation frequencies in a cloudless atmosphere and in continental boundary layer clouds. *J. Geophys. Res.*, **105**, 9843–9857.

Joseph, J. H., W. J. Wiscombe, and J. A. Weinman, 1976: The delta-Eddington approximation for radiative transfer flux. *J. Atmos. Sci.*, **33**, 2452–2458.

Lenderink, G., A. P. Siebesma, S. Cheinet, S. Irons, C. G. Jones, P. Marquet, F. Muller, D. Olmeda, J. Calvo, E. Sanchez, and P. M. M. Soares, 2005: The diurnal cycle of shallow cumulus over land: a single column model intercomparison study. *Quart. J. Roy. Meteorol. Soc.*, **123**, 223–242.

Madronich, S., 1987: Photodissociation in the atmosphere: 1. Actinic fluxes and the effects of ground reflections and clouds. *J. Geophys. Res.*, **92**, 9740–9752.

Moeng, C.-H., 1984: A large-eddy simulation model for the study of planetary boundary-layer turbulence. *J. Atmos. Sci.*, **41**, 2052–2062.

Molemaker, M. J. and J. Vilà-Guerau de Arellano, 1998: Turbulent control of chemical reactions in the convective boundary layer. *J. Atmos. Sci.*, **55**, 568–579.

Patton, E. G., P. P. Sullivan, and C.-H. Moeng, 2005: Influence of idealized heterogeneity on wet and dry planetary boundary layers coupled to the land surface. *J. Atmos. Sci.*, **62**, 2078–2097.

Schumann, U., 1989: Large-eddy simulation of turbulent diffusion with chemical reactions in the convective boundary layer. *Atmos. Environ.*, **23**, 1713–1729.

Siebesma, A. P. and J. W. M. Cuijpers, 1995: Evaluation of parametric assumptions for shallow cumulus convection. *J. Atmos. Sci.*, **52**, 650–666.

Stephens, G., 1984: The parameterization of radiation for numerical weather prediction and climate models. *Mon. Wea. Rev.*, **112**, 826–867.

Sullivan, P. P., J. C. McWilliams, and C.-H. Moeng, 1996: A grid nesting method for large-eddy simulation of planetary boundary-layer flows. *Bound.-Layer Meteorol.*, **80**, 167–202.

van Weele, M. and P. G. Duynkerke, 1993: Effects of clouds on the photodissociation of NO_2: observations and modelling. *J. Atmos. Chem.*, **16**, 231–255.

Vilà-Guerau de Arellano, J. and J. W. M. Cuijpers, 2000: The chemistry of a dry cloud: the effects of radiation and turbulence. *J. Atmos. Sci.*, **57**, 1573–1584.

Vilà-Guerau de Arellano, J., S. W. Kim, M. C. Barth, and E. G. Patton, 2005: Transport and chemical transformations influenced by shallow cumulus over land. *Atmos. Chem. Phys.*, **5**, 3219–3231.

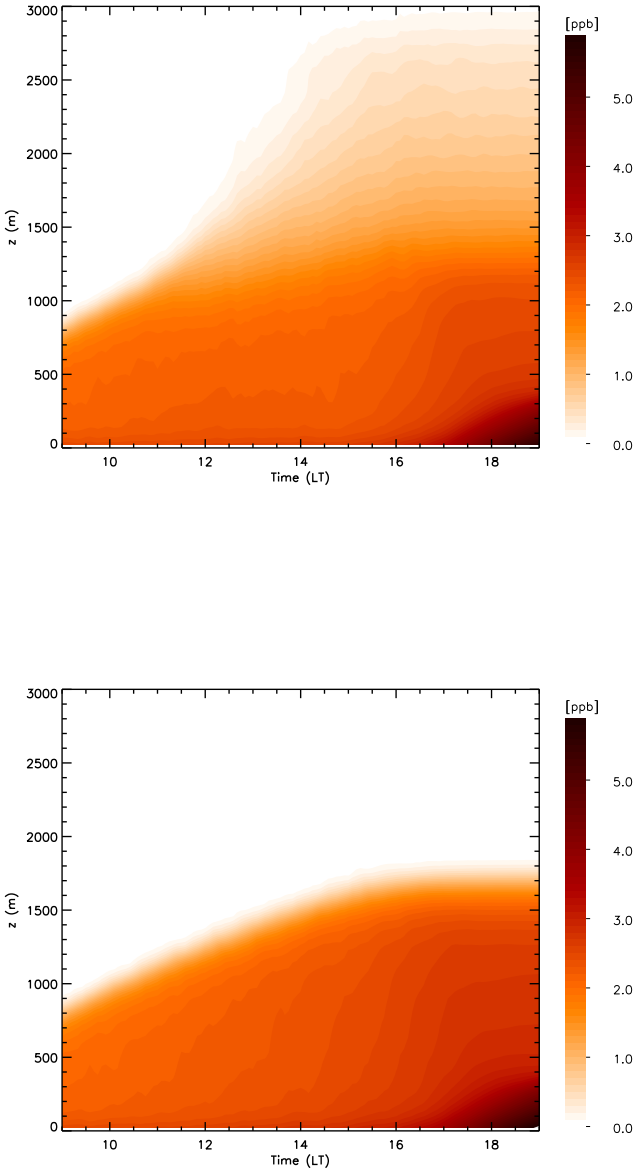

FIG. 1: *Time evolution of the inert atmospheric compounds (a) in the cloud situation CL and (b) in the clear sky situation CS. Shallow cumulus begin to form around 10 LT.*

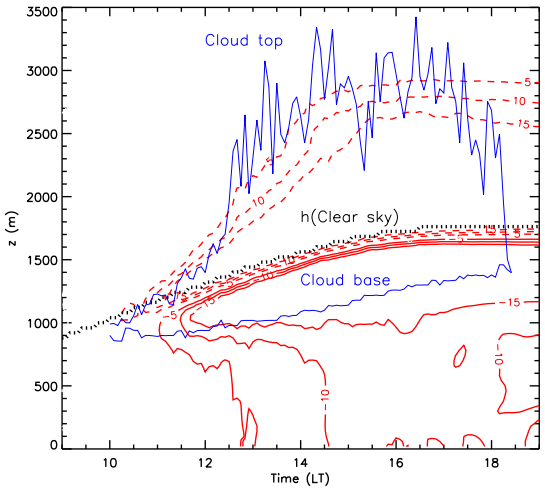

FIG. 2: *Dimensionless difference of the inert scalar mixing ratio between the cloud situation (CL) and the clear sky situation (CS): $100(CL - CS)/(< CS >)$ (red), where $< CS >$ is the mixing ratio volume averaged in the CS situation. The evolution of the cloud top and cloud base height (CL case) (blue) and the CS boundary layer height (black) is also shown.*

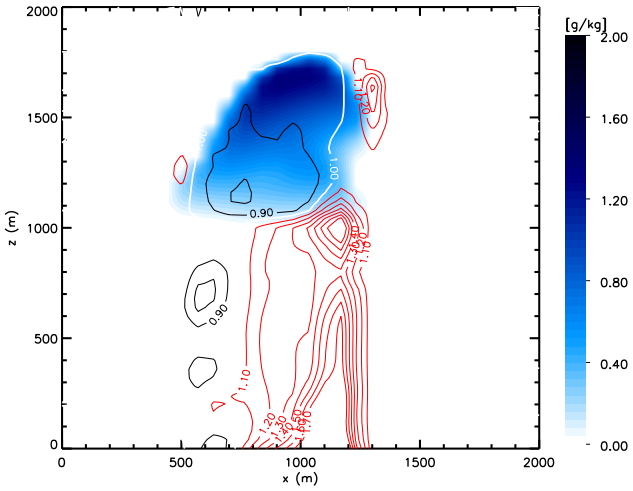

FIG. 3: *Vertical cross section of the liquid water content (blue) and the photostationary state (Φ) calculated from the instantaneous mixing ratio when shallow cumulus were more active (between 15-16 LT). At chemical equilibrim Φ=1. Values lower than 1 are in red. Values higher than 1 are in black.*